Supplementary Information (SI) for RSC Mechanochemistry.

Supporting Information

Why are zeolites harder to make than MOFs? A study of the sodalite system

Haochen Wu[a], Daniel N. Rainer[b], Simon J. Coles[b], Samuel J. Page[c], Stuart L. James[a]*

[a] School of Chemistry and Chemical Engineering, Queen's University Belfast, Belfast, BT9 5AG, UK

[b] School of Chemistry and Chemical Engineering, Faculty of Engineering and Physical Sciences, University of Southampton, Southampton, SO17 1BJ, UK

[c] School of Chemistry, Solid-state NMR Service, Durham University, Durham, DH1 3LE, UK

Content

1. Materials and synthesis methods

1.1 Materials

All materials were purchased from Sigma Aldrich and were used as obtained.

1.2 Synthesis methods

Synthesis from alkoxylsilanes

(1) Precursor synthesized by mixing: $Al(OAc)_2OH$ (0.39 g, 2.40 mmol), NaOH (0.29 g, 7.21 mmol) and organosilane (2.40 mmol, in the case of TEOS, 0.50 g; VTEOS, 0.46 g; PTEOS, 0.58 g) were added to a Teflon-liner and mixed manually for 3-5 minutes. This corresponds to a precursor molar ratio of: Al: Si: Na = 1.00: 1.00: 3.00. The excess amount of the NaOH is mainly to accelerate the reaction. The resulting white powder was transferred to a Teflon-lined stainless-steel autoclave and heated at 180 °C for 4 or 24 h. The resulting crude product was rinsed 5 times with double-deionised water (40 ml), collected by centrifugation repeatedly at 4000 rpm for 10 minutes until the supernatant was neutral, and air dried at room temperature overnight. The resulting samples were denoted as TSOD, VSOD, PSOD, respectively.

(2) Precursor synthesized by ball-milling: $Al(OAc)_2OH$ (0.39 g, 2.40 mmol), NaOH (0.29 g, 7.21 mmol) and TEOS (0.50 g, 2.40 mmol) were added to a Teflon ball-milling jar with two Teflon balls (ϕ12 mm, 5.5 g each) and milled at 23.3 Hz for 50 minutes. This corresponds to a precursor molar ratio of: Al: Si: Na = 1.00: 1.00: 3.00. The excess amount of the NaOH is mainly to accelerate the reaction. The obtained whitish powder was transferred to a Teflon-lined stainless-steel autoclave and heated at 180 °C for 24 or 48 h. The resulting crude product was rinsed 5 times with double deionised water (40 ml), collected by centrifugation repeatedly at 4000 rpm for 10 minutes until the supernatant was neutral, and air dried at room temperature overnight.

Synthesis from $Na_2SiO_3 \cdot 5H_2O$

$Al(OAc)_2OH$ (0.39 g, 2.40 mmol) and $Na_2SiO_3 \cdot 5H_2O$ (1.51 g, 7.10 mmol) were added to a Teflon-liner and mixed manually for 3–5 min. This corresponds to a precursor molar ratio of: Al: Si: Na: H_2O = 1.00: 2.96: 5.92: 14.79. The excess amount of the NaOH is mainly to accelerate the reaction. Then, it was transferred to a Teflon-lined stainless-steel autoclave and heated at 100-300 °C for 0.5-4.0 h. The resulting crude product was washed with double deionised water (40 ml, 4 times), collected by centrifugation at 4000 rpm for 10 minutes repeatedly until the supernatant was neutral and air dried at room temperature overnight.

2. Instruments and characterization

2.1 Instruments

X-ray diffraction patterns were measured at room temperature using a PANanalytical X'Pert Pro X-ray diffractometer with CuKα radiation (λ = 1.5405 Å) and Bruker D8 Advance eco XRD with a Cu Kα anode (λ = 1.5405 Å) operating at 40 kV and 30 mA. Nitrogen adsorption isotherms were collected at 77 K up to $P/P_0 = 0.95$ using a Quantachrome Nova 4200e Surface Area Analyzer. The specific surface area was calculated by applying the Brunauer–Emmett–Teller (BET) method to the linear region of the isotherm ($P/P_0 = 0.05$–0.35). Scanning electron microscopy (SEM) was performed using a JEOL JSM-6500F microscope. Particle size measurements were taken from two to three different sites and determined using the software's scale function, with the recorded diameter range defined by the smallest and largest observed particles. The thermogravimetric analysis (TGA) was performed in accordance with the standard procedure of the Analytical Services and Environmental Projects (ASEP) Department, Queen's University Belfast, using a heating rate of 2 $°C\cdot min^{-1}$ under a nitrogen atmosphere up to 1000 °C.

Ball milling: Experiments were performed on a Retsch MM 400 mixer mill operated from 5 to 30 Hz. The milling jar is interchangeable and can be PTFE (Teflon), zirconia, or stainless steel, with matching media.

TSE: Twin-screw extrusion. Experiments were performed on a Tree-tech ZE 12 HMI co-rotating twin-screw extruder. The screws are housed in a split stainless-steel barrel. The upper and lower halves clamp together for operation and can be separated for cleaning. The barrel has six temperature-controlled zones with thermocouples and a 30–200 °C set-point range. The maximum screw speed is 300 rpm. The drive delivers up to 12 N·m torque. During runs, torque below 10 N·m indicates normal loading. A sustained rise toward the limit signals potential blockage and the run should be stopped.

2.2 PXRD based calculations

Crystallinity

This calculation is based on the ratio of the sum of the areas under the individual diffraction peaks corresponding to the SOD crystalline phase to the total area under the diffraction curve within the specified range for SOD. Crystallinity was calculated using the following formula:

$$Crystallinity\ (\%) = \frac{\sum individual\ peak\ area\ of\ SOD}{\sum Total\ area\ under\ the\ diffraction\ curve} \times 100\%$$

The crystallinity was determined by repeatedly measuring the individual peak areas of SOD and the total area under the diffraction curve, with five manual measurements performed. The mean crystallinity was subsequently calculated, and the standard deviation was found to be typically less than 3%.

SOD simulation pattern

The simulated powder X-ray diffraction (PXRD) patterns were generated using the Mercury software (version 4.0.0, developed by the Cambridge Crystallographic Data Centre, CCDC). The crystal structure data, provided in CIF format, was obtained from the Zeolite Structure Database. Using this data, diffraction patterns were simulated by applying

Bragg's Law and calculating structure factors, with Gaussian peak broadening applied to account for instrumental and sample-related effects.

2.3 Electron diffraction

All data collections were performed on an XtaLAB SynergyED (LaB_6, 200 kV) with HyPix-ED detector in continuous rotation mode using a selected area aperture (~2 µm in the image plane) under optimised beam conditions. A carbon coated copper TEM grid (Agar Scientific, 200 mesh) were used (lacey carbon for TSOD, holey carbon for VSOD). The grid for TSOD was prepared dry by lightly grinding and dispersing the white, solid powder between microscopy glass slides and dabbing the grid in the solid. For VSOD (white, solid powder) the grid was placed in the vial containing the sample and the vial manually shaken. The grids were mounted on a Gatan Elsa cryogenic holder and introduced into the column using cryo transfer at 175(5) K, and data collections were also performed at this temperature. All data were collected using CrysAlisPRO (version 1.171.43.118a, Oxford Diffraction Ltd., Yarnton, Oxfordshire, England).

For both samples, data was collection from several particles, all indexable in a cubic unit cell. It is possible to index in a body centred cell, however, in line with literature,[1] a cubic primitive cell was chosen, allowing structure solution in space group *P*-43*n*, where the silicon and aluminum framework atoms can occupy a separate position each (a Si/Al ratio of 1 is assumed based on synthesis). For the final dataset, several individual data collections were chosen (5 for TSOD, 3 for VSOD), individually indexed and integrated, and subsequently merged and scaled together for each model using CrysAlisPRO (version 1.171.44.98a for VSOD and 1.171.44.47a for TSOD, Oxford Diffraction Ltd., Yarnton, Oxfordshire, England) and SCALE3 ABSPACK, implemented therein.

The structures were solved using SHELXT,[2] and refined in the kinematic approximation using SHELXL as implemented in Olex2 (version 1.5-ac7-014, compiled 2025.02.27 svn.r6f4c0eaf for Rigaku Oxford Diffraction, GUI svn.r7171)[3] using published scattering factors.[4] The refinement was performed employing the kinematical approximation and using an extinction correction parameter to broadly account for dynamical effects.
After refining the framework atoms (Si, Al, O), distinct maxima in the residual electrostatic potential (2 for VSOD, 3 for TSOD) were assigned to sodium and their combined occupancy effectively constrained to the occupancy of aluminium, balancing the negative charge associated with the aluminosilicate zeolite framework. Some thermal restraints had to be applied to achieve physically sensible AADPs.

Complete experimental and refinement information are contained in the deposited CIFs along with structure factors and embedded .RES files. These are deposited in the CSD with CSD reference codes CSD 2432426 (TSOD) and 2432427 (VSOD). **Tables S1** and **Table S2** report experimental parameters from the merged refinement and individual datasets for TSOD and VSOD, respectively.

Table S1| Crystal data and structure refinement for TSOD.

	Merged Crystal Data				
Identification code	TSOD, 2024NCS0186				
CSD number	2432426				
Chemical formula	SiAlO4Na				
M_r	142.05				
Crystal system, space group	Cubic, $P-43n$				
Temperature (K)	175(5)				
a, b, c (Å)	9.0311(7), 9.0311(7), 9.0311(7)				
α, β, γ (°)	90, 90, 90				
V (Å^3)	736.58(17)				
Z	6				
Radiation type	Electron, λ = 0.02510 Å				
No. Crystals	5				
	Distinct Data Collections				
a = b = c (Å)	9.0685(16)	9.0282(16)	9.0247(14)	9.0319(12)	9.0274(16)
$\alpha = \beta = \gamma$ (°)	90	90	90	90	90
V (Å^3)	745.8(2)	735.9(2)	735.0(2)	736.77(17)	735.7(2)
h (min, max)	-11, 11	-10, 10	-11, 11	-11, 11	-11, 11
k (min, max)	-10, 10	-11, 11	-10, 10	-11, 11	-10, 11
l (min, max)	-10, 10	-11, 11	-11, 11	-9, 10	-11, 11
	Merged dataset				
No. reflections (meas., indep., obs [I ≥ 2u(I)])	8931, 257, 161				
R_{int}	0.2499				
2Θ range for data collection (°)	0.226 to 1.788				
h (min, max)	-11, 11				
k (min, max)	-11, 11				
l (min, max)	-11, 11				
	Refinement				
R_1, wR_2, [$F^2 > 2\sigma(F^2)$]	0.1554, 0.3633				
R_1, wR_2, [all]	0.1784, 0.4033				
Goodness-of-fit on F^2	1.059				
Data/restraints/parameters	257/22/30				
$\Delta\varphi_{max}$, $\Delta\varphi_{min}$ (as output by SHELXL)	0.25, -0.16				

Table S2| Crystal data and structure refinement for VSOD.

	Merged Crystal Data		
Identification code	VSOD, 2024NCS0187		
CSD number	2432427		
Chemical formula	SiAlO4Na		
M_r	142.05		
Crystal system, space group	Cubic, *P*−43*n*		
Temperature (K)	175(5)		
a, *b*, *c* (Å)	9.0718(9), 9. 0718(9), 9. 0718(9)		
α, β, γ (°)	90, 90, 90		
V (Å^3)	746.6(2)		
Z	6		
Radiation type	Electron, λ = 0.02510 Å		
No. Crystals	3		
	Distinct Data Collections		
a = b = c (Å)	9.074(3)	9.0791(10)	9.063(2)
α = β = γ (°)	90	90	90
V (Å^3)	747.0(5)	748.38(14)	744.4(3)
h (min, max)	-11, 11	-11, 11	-11, 11
k (min, max)	-11, 11	-10, 10	-11, 11
l (min, max)	-10, 10	-10, 10	-11, 11
	Merged dataset		
No. reflections (meas., indep., obs [I ≥ 2u(I)])	10280, 261, 184		
R_{int}	0.5615		
2Θ range for data collection (°)	0.224 to 1.8		
h (min, max)	-11, 11		
k (min, max)	-11, 11		
l (min, max)	-11, 11		
	Refinement		
R_1, wR_2, [$F^2 > 2\sigma(F^2)$]	0.1831, 0.4271		
R_1, wR_2, [all]	0.2034, 0.4606		
GoF(*S*) (inc., exlc. restraints)	1.045		
Data/restraints/parameters	261/40/25		
$\Delta\varphi_{max}$, $\Delta\varphi_{min}$ (as output by SHELXL)	0.72, -0.22		

2.4 ^{27}Al MAS NMR spectroscopy

^{27}Al magic-angle spinning (MAS) NMR measurements were carried out with a 3.2 mm (rotor o.d.) probe. All data was recorded using a Bruker Avance III HD spectrometer operating at 104.3 MHz for ^{27}Al. Spectra were acquired at a spin rate of 20 kHz. All direct excitation ^{27}Al spectra were acquired with a 1 μs 30 degree solid pulse which was determined from a 9 µs solution pulse determined on 1M $Al(NO_3)_3$. The spectra were acquired with a recycle delay of 1 s determined on the sample. Aluminium spectral referencing is relative to 1M $Al(NO_3)_3$ carried out by setting the signal to 0.0 ppm.

2.5 ^{13}C MAS NMR spectroscopy

^{13}C MAS NMR measurements were carried out at 100.63 MHz using a Bruker Avance III HD spectrometer and 4 mm (rotor o.d.) probe. Spectra were acquired at a spin rate of 10 kHz. Cross-polarisation (CP) spectra were recorded with TOSS spinning sideband suppression, 1-4 ms contact time. Carbon spectral referencing is relative to neat tetramethyl silane, carried out by setting the high frequency signal from an external sample of adamantane to 38.5 ppm

3. Figures and Tables

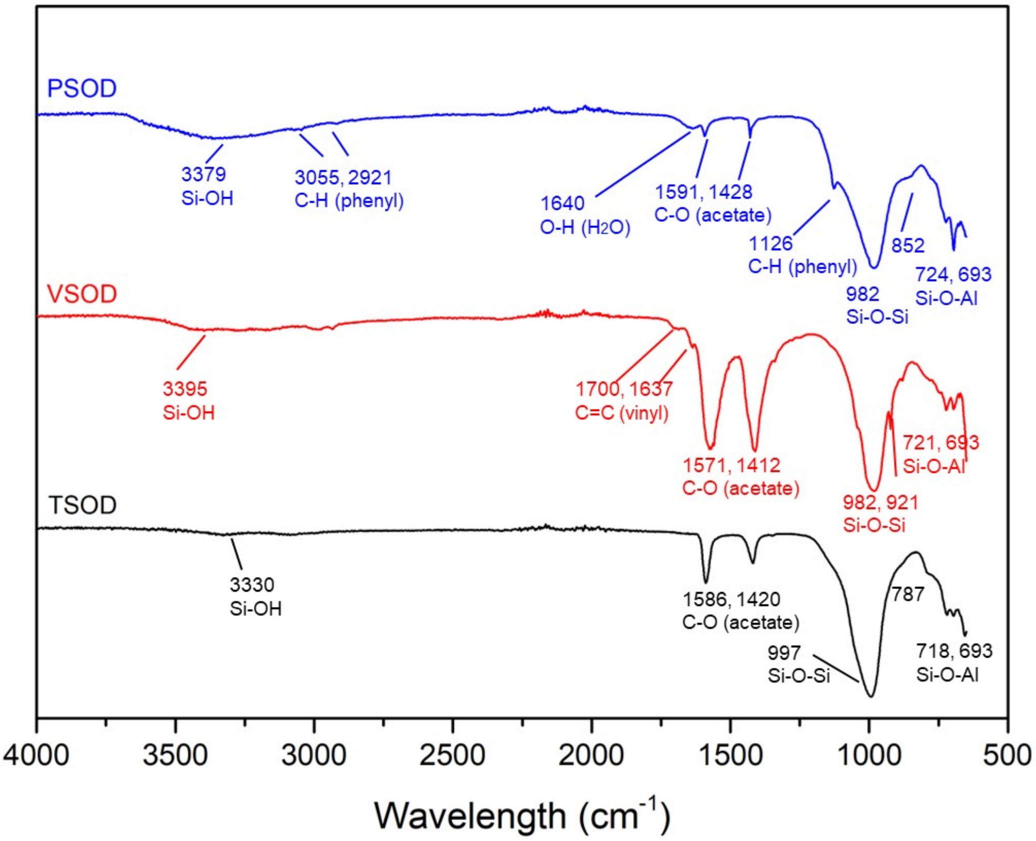

Figure S1 | Infrared spectra of synthesized TSOD, VSOD and PSOD

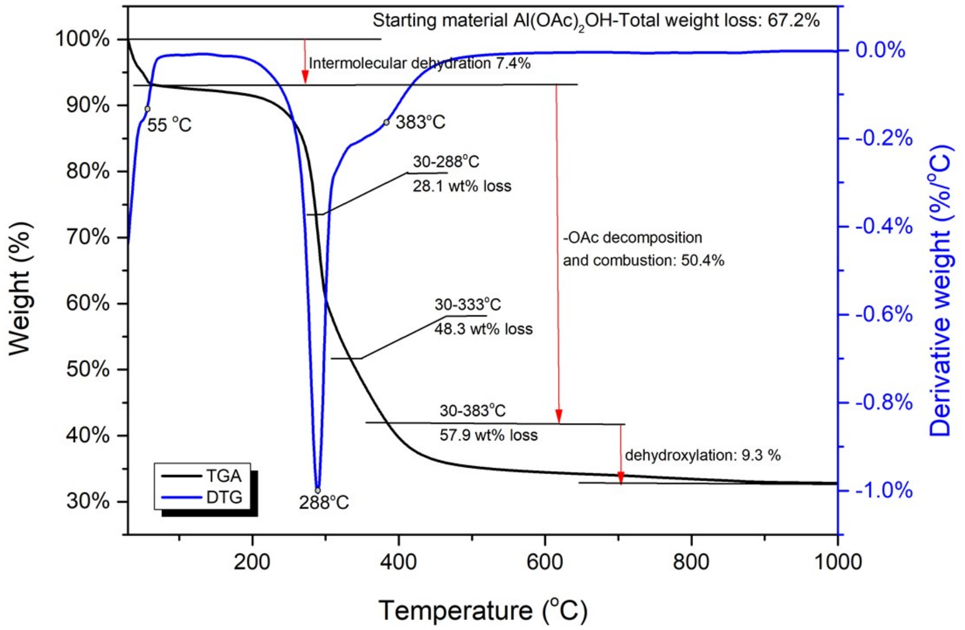

Figure S2 | Weight % remaining as a function of temperature determined by TGA for starting material Al(OAc)$_2$OH.

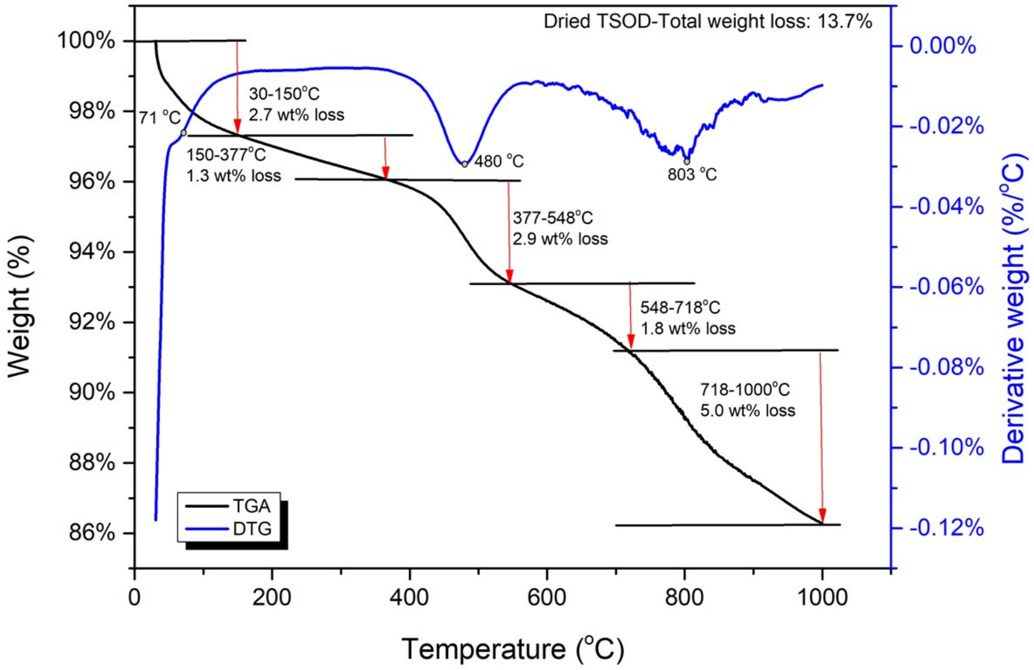

Figure S3 | Weight % remaining as a function of temperature determined by TGA for the synthesized TSOD.

Table S3| TGA result of $Al(OAc)_2OH$ and TSOD in temperature range of 30-1000°C with theoretical/ actual weight-loss

Compound	Temperature range	Process	Theoretical step weight-loss (wt%)	Actual step weight-loss (wt%)	Theoretical total weight-loss (wt%)	Actual total weight-loss (wt%)
$Al(OAc)_2OH$	30-63°C	Intermolecular dehydration	5.6	7.4	5.6	7.4
	63-383 °C	Acetate decomposition	51.9	50.4	57.4	57.9
	383-1000 °C	Dehydroxylation	11.1	9.3	68.6	67.2
TSOD	30-150°C	SOD adsorbed water dehydration	[a, e]~1-3	2.7	[a, e]~1-3	2.7
	150-377 °C	SOD crystalline water dehydration	[a, e] ~4	1.3	[a, e]~5-7	4.0
	377-548 °C	Acetate decomposition	[b]1.6-[c]2.4	2.9	[d]3.9-4.2	[d]4.7
	548-718 °C	Acetate decomposition	[c]1.8-[b]2.6	1.8		
	718-900 °C	Dehydroxylation+	[e] ~2	3.8	~10.9-13.2	13.7
	900-1000 °C	SOD structural water		1.2		

[a] Reference to Khajavi *et al.*'s work[5]; [b] Refer to elemental analysis data of TSOD calcined at 550°C for 4h sample; [c] Refer to elemental analysis data of TSOD calcined at 550°C for 10h sample; [d] Excludes zeolite adsorbed water and crystalline water (i.e., only acetate decomposition is considered); [e] Reference to Makgaba *et al.*'s work[6]

During the step of intermolecular dehydration between two $Al(OAc)_2OH$ molecules, the obtained actual weight-loss is 7.4% (theoretical 5.6%), where the more weight-loss maybe due to the adsorbed water and the early stage of acetate decomposition. The acetate decomposition step is observed as losing 50.4% weight compared to the theoretical weight-loss of 51.9% and the DTG curve showing a small hump around 383°C, indicating the ending stage of acetate decomposition. A relatively lower weight-loss (9.3% compared to 11.1%) is observed in dehydroxylation step, where a longer heating time may be needed. However, a more complicated case is shown in the TSOD TGA because the adsorbed, crystalline, and structural water are present in TSOD structure. Compared to the reported SOD synthesis without inorganic salt and organic template,[5, 6] the typical adsorbed water is of ~1-3% (< 150°C), while crystalline water is ~4% (150-377°C), and ~2 % of structural water are removed at 718-1000°C. The observed adsorbed and crystalline water content is counted in total of 4%, which is lower than the theoretical weight loss (5-7%). A reasonable explanation is the impregnated acetate containing species such as $Al(OAc)^{2+}$ and $Al(OAc)OH^{+}$ occupied the sodalite cage, hence less water can be accommodated in. The decomposition of acetate group in the TSOD case generally requires higher temperature as the pore size of SOD (2.9 Å) is smaller than the CO_2 kinetic diameter (3.3 Å), which limited the CO_2 mobility and further leads to a lower removing rate (~0.02 vs 0.2 wt%/°C).

Table S4 | Elemental analysis of the SOD synthesis

Compound	Element (wt%)				Chemical ratio	Proposed Chemical formula
	Al	Si	C	H		
TSOD (air dried)	18.62	14.90	3.57	0.66	$Si_{4.5}Al_{5.9}C_{2.5}H_{5.6}$	$[Al_3Si_3O_{12}]_2[Na_2Al(OAc)OH]_2$
TSOD (calcined 4h)	19.30	16.97	2.30	0.30	$Si_{5.2}Al_{6.1}C_{1.6}H_{2.5}$	-
TSOD (calcined 10h)	19.20	16.38	1.53	0.30	$Si_{5.0}Al_{6.1}C_{1.1}H_{2.5}$	-
VSOD (calcined)	16.33	17.65	2.17	0.98	$Si_{5.4}Al_{5.2}C_{1.5}H_{8.3}$	-
PSOD (calcined)	17.96	17.21	1.38	0.92	$Si_{5.2}Al_{5.7}C_{1.0}H_{7.8}$	-
QSOD Scale-up (air dried)	12.99	14.78	4.38	0.50	$Si_{4.5}Al_{4.1}C_{3.1}H_{4.2}$	$[Al_3Si_3O_{12}]_2[Na_4(OAc)]_2$

Table S5 | The reported SOD synthesis method and in this study

Method	Starting materials	Temp.	Time	PXRD crystallinity	BET surface area	Reference
Hydrothermal	NaOH, $NaSiO_3$ and $NaAlO_2$	363-413 K	3.5-24 h	High	27.4 m^2/g	[5, 7]
	Coal fly ash and NaOH	368 K	24 h	Medium	33.0 m^2/g	[8]
	$NaSiO_3·9H_2O$, $Al(OH)_3$ and NaOH	463-563 K	3 h	High	5.5-41.1 m^2/g	[9]
Solventless	$NaSiO_3·9H_2O$, $NaAlO_2$	353 K	10-20 h	Medium	35.7 m^2/g	[10]
	$NaSiO_3·9H_2O$ and AlOOH	353 K	12 h	Medium	42.9 m^2/g	[11]
	TEOS, $Al(OAc)_2OH$ and NaOH	453 K	4 or 24 h	Medium-High	34.0 m^2/g	This work
	$NaSiO_3·5H_2O$ and $Al(OAc)_2OH$	423-573 K	0.5-4 h	High	10.5-42.4 m^2/g	This work

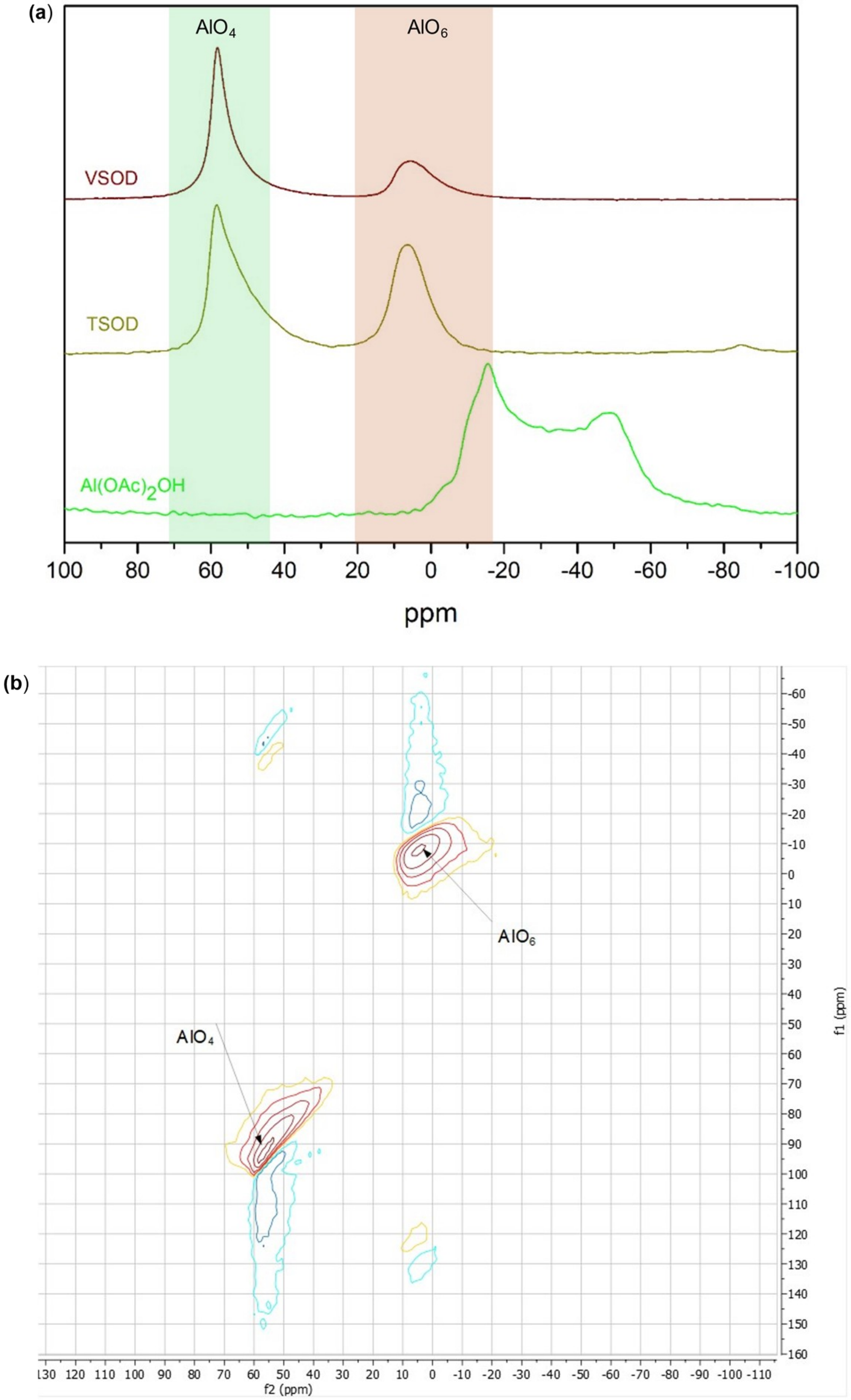

Figure S4 | (a) ^{27}Al MAS NMR spectra of $Al(OAc)_2OH$, TSOD and VSOD, (b) MQMAS NMR of the TSOD.

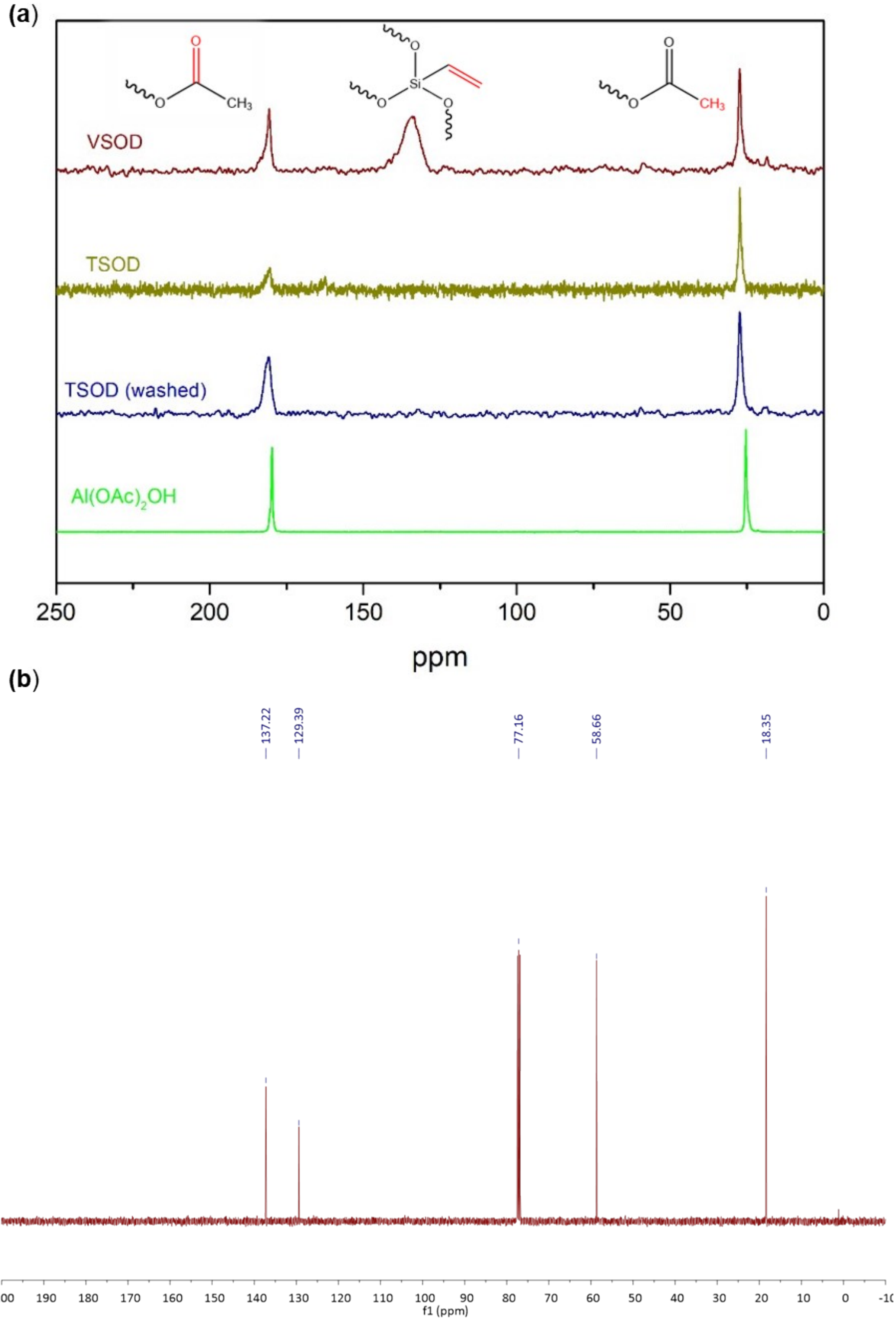

Figure S5 | (a) ^{13}C MAS NMR spectra of $Al(OAc)_2OH$, TSOD (washed), TSOD and VSOD. (b) ^{13}C NMR of the VTEOS using $CDCl_3$ as the solvent.

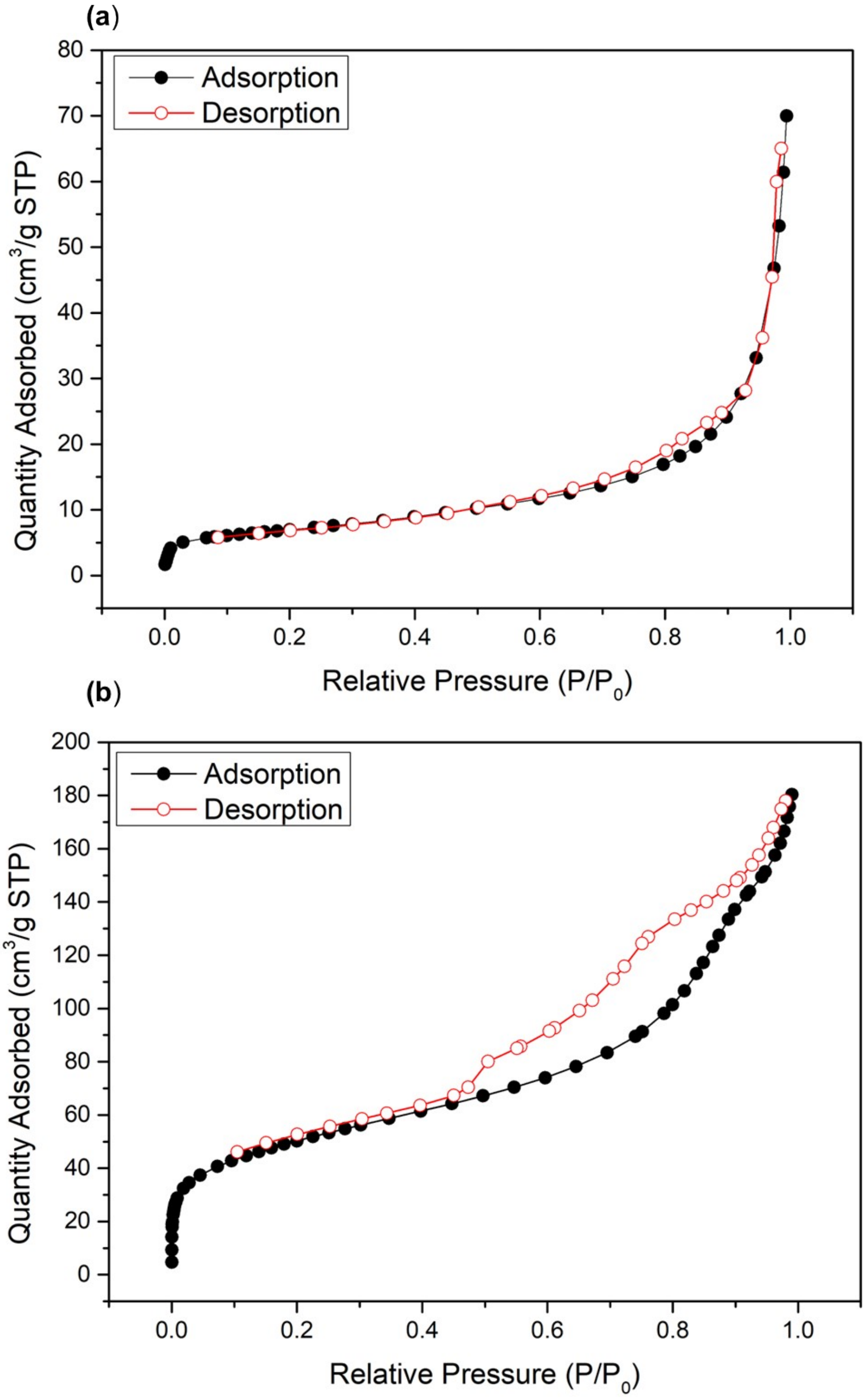

Figure S6 | N_2 isotherm of (a) TSOD as synthesized, (b) VSOD as synthesized.

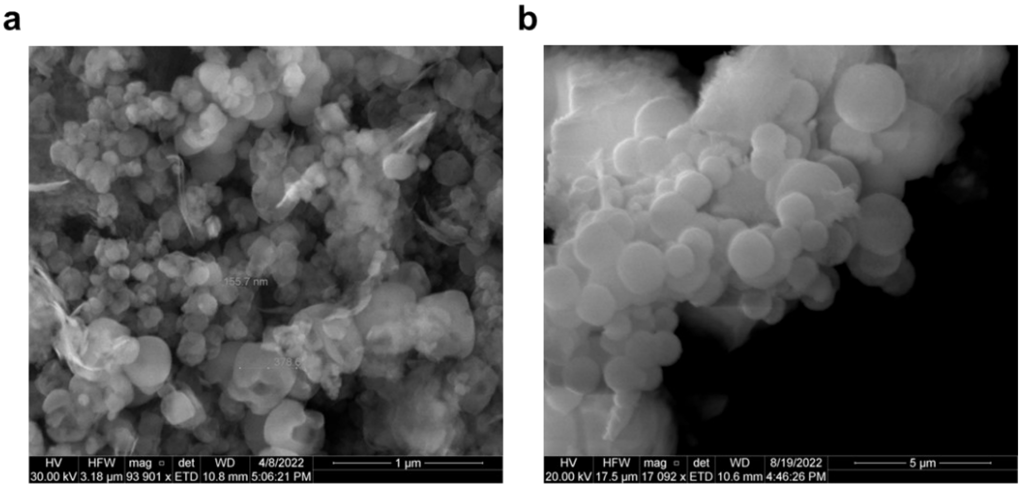

Figure S7 | SEM images of (a) TSOD synthesized by 24 h reaction at 180 ^{o}C and (b) VSOD

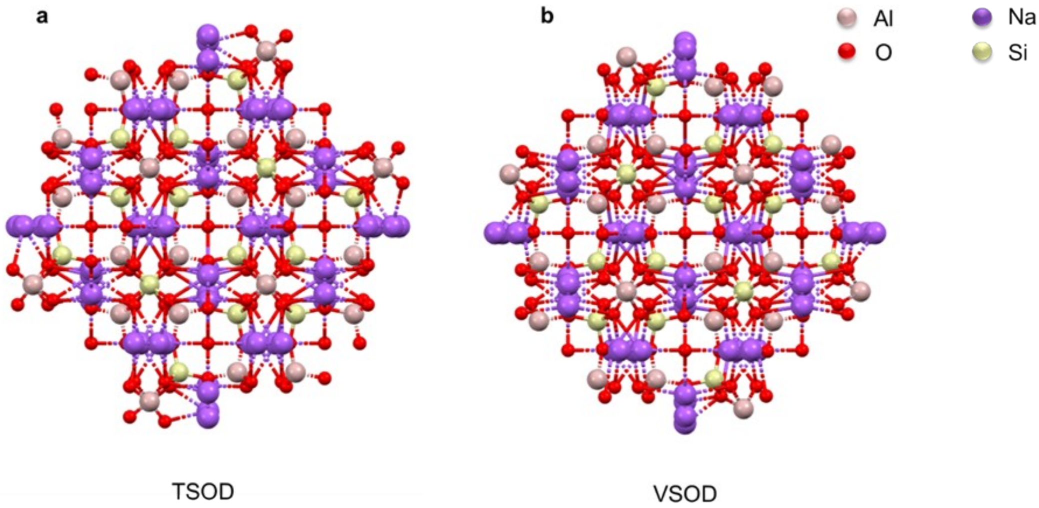

Figure S8 | The crystal structure of **(a)** TSOD synthesized by 24 h reaction at 180 ^{o}C, and **(b)** VSOD

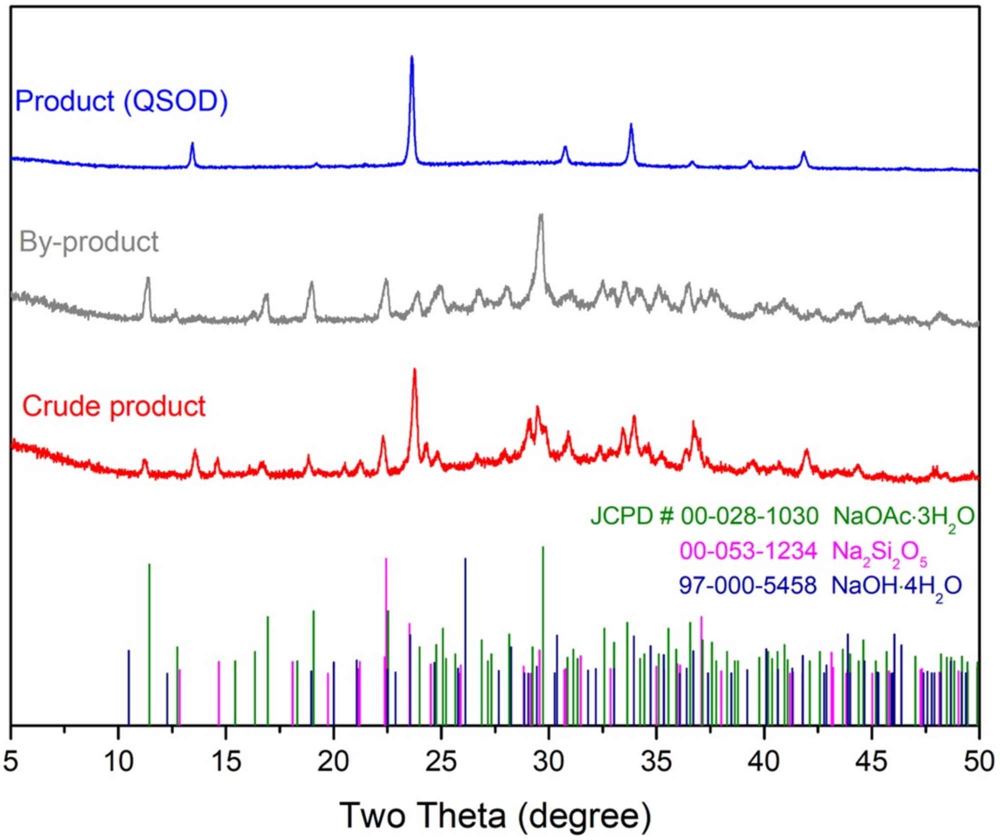

Figure S9 | PXRD pattern of product, by-product, and crude product with corresponding JCPDS references.

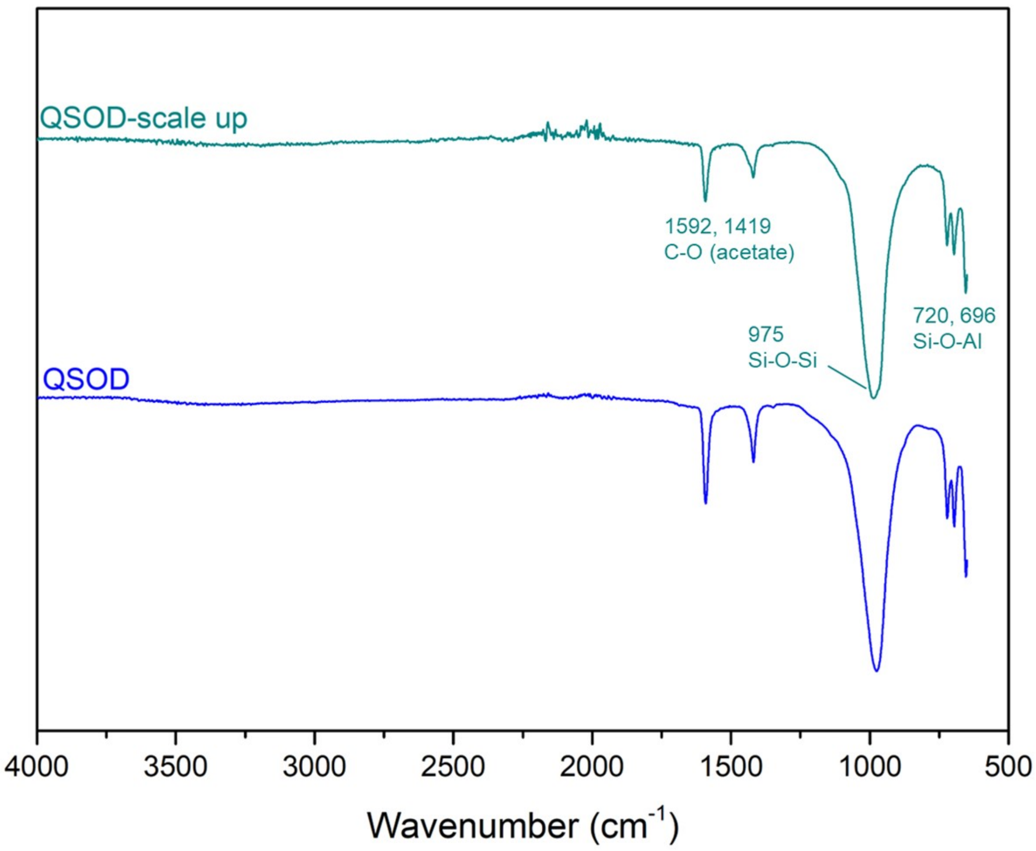

Figure S10 | Infrared spectrum of the synthesized QSOD and QSOD-scaleup

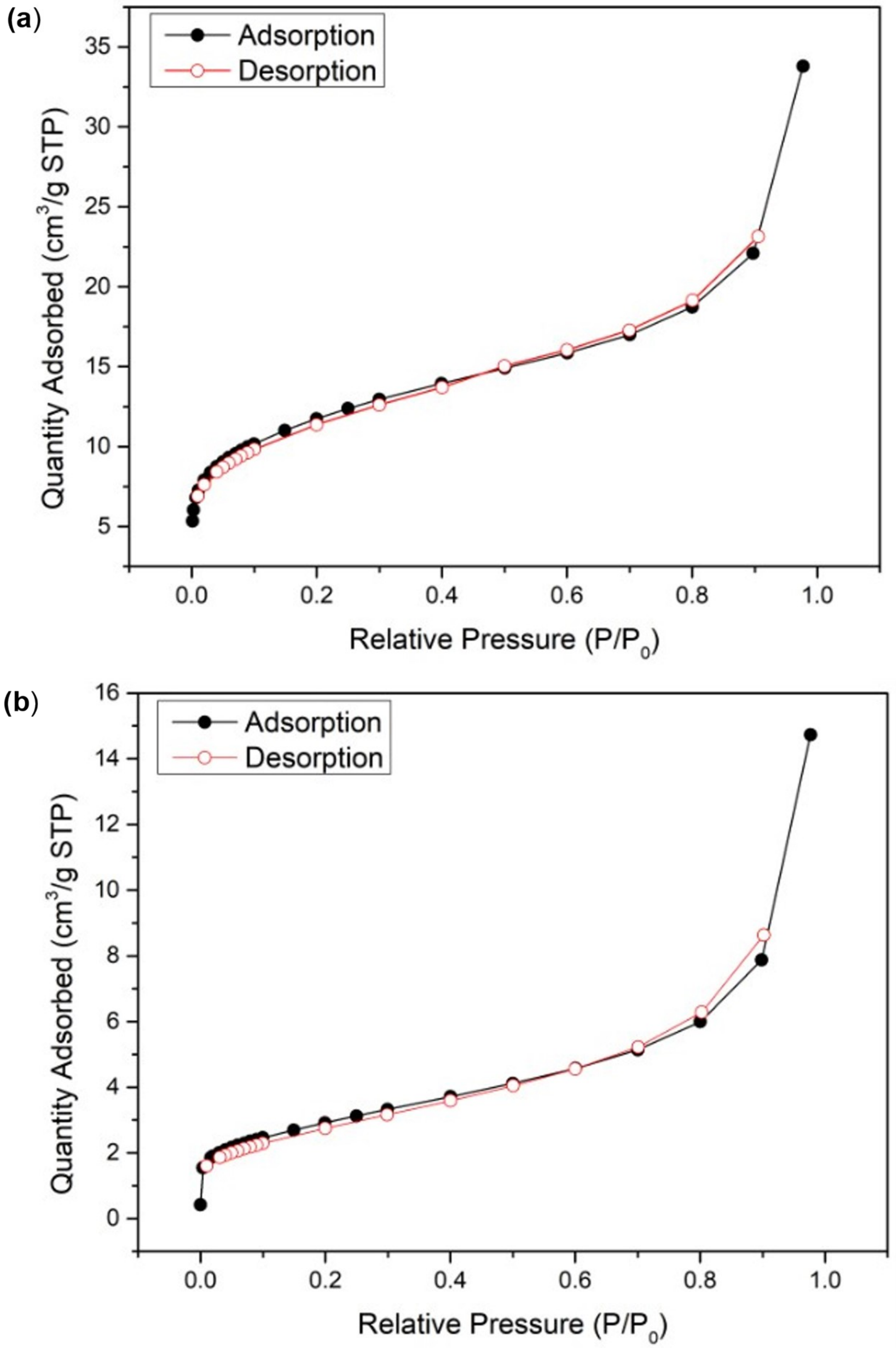

Figure S11 | N_2 adsorption-desorption isotherm of **(a)** QSOD as synthesized, **(b)** QSOD-scaleup as synthesized.

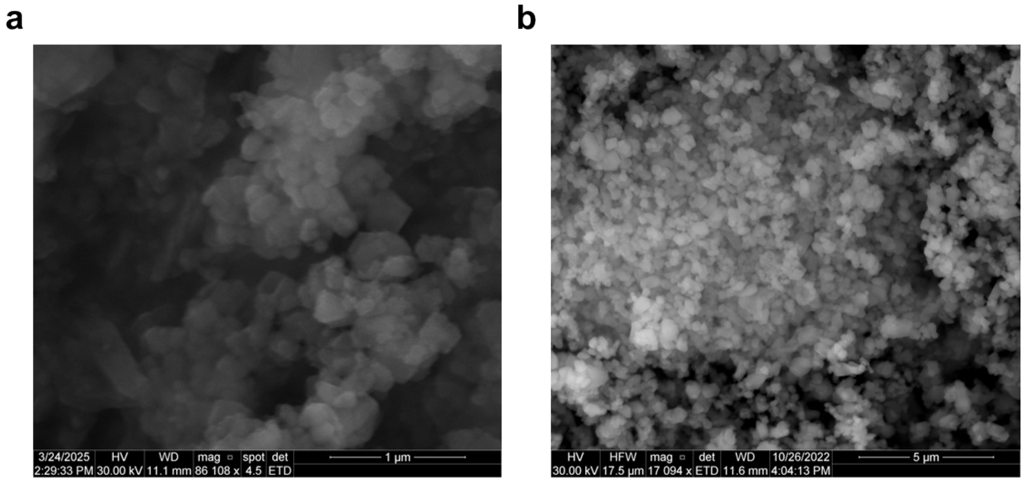

Figure S12 | SEM images of (a) QSOD and (b) QSOD-scale up

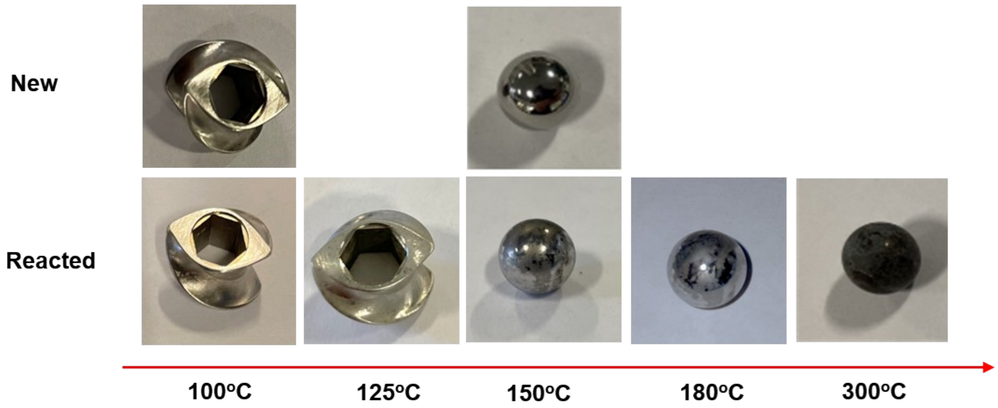

Figure S13 | Image of new steel component and after heating with starting materials at 100-300°C for 4 hours

Figure S14 | Image of new ball milling jar and after milling with starting materials at 23.3 Hz for 50 minutes

References

1. J. Löns and H. Schulz, *Acta Crystallographica*, 1967, **23**, 434-436.
2. G. M. Sheldrick, *Acta Crystallogr. A*, 2015, **71**, 3-8.
3. O. V. Dolomanov, L. J. Bourhis, R. J. Gildea, J. A. K. Howard and H. Puschmann, *Applied Crystallography*, 2009, **42**, 339-341.
4. A. Saha, S. S. Nia and J. A. Rodríguez, *Chemical Reviews*, 2022, **122**, 13883-13914.
5. S. Khajavi, S. Sartipi, J. Gascon, J. C. Jansen and F. Kapteijn, *Microporous and Mesoporous Materials*, 2010, **132**, 510-517.
6. C. P. Makgaba, T. C. Aniokete and M. O. Daramola, *Progress in Industrial Ecology, an International Journal*, 2018, **12**, 331-344.
7. C. L. Eden and M. O. Daramola, *Materials Today: Proceedings*, 2021, **38**, 522-527.
8. W. Franus, M. Wdowin and M. Franus, *Environmental Monitoring and Assessment*, 2014, **186**, 5721-5729.
9. X. Jiang, Y. Zhang and Y. Zhang, *Reaction Kinetics, Mechanisms and Catalysis*, 2019, **127**, 489-504.
10. S. Zeng, R. Wang, A. Li, W. Huang, Z. Zhang and S. Qiu, *CrystEngComm*, 2016, **18**, 6779-6783.
11. S. Khajavi, J. C. Jansen and F. Kapteijn, *Journal of Membrane Science*, 2009, **326**, 153-160.